C-doped ZnO nanowires: Electronic structures, magnetic properties, and a possible spintronic device

Zhenxiang Dai,[1] Argo Nurbawono,[1] Aihua Zhang,[1] Miao Zhou,[1] Yuan Ping Feng,[1] Ghim Wei Ho,[2] and Chun Zhang[1,3,a)]

[1]*Department of Physics, National University of Singapore, 2 Science Drive 3, Singapore 117542*
[2]*Department of Electrical and Computer Engineering, National University of Singapore, 4 Engineering Drive 3, Singapore 117576*
[3]*Department of Chemistry, National University of Singapore, 3 Science Drive 3, Singapore 117543*

Electronic structures, magnetic properties, and spin-dependent electron transport characteristics of C-doped ZnO nanowires have been investigated via first-principles method based on density functional theory and nonequilibrium techniques of Green's functions. Our calculations show that the doping of carbon atoms in a ZnO nanowire could induce strong magnetic moments in the wire, and the electronic structures as well as the magnetic properties of the system sensitively depend on partial hydrogenation. Based on these findings, we proposed a quasi-1d tunneling magnetic junction made of a partially hydrogenated C-doped ZnO nanowire, which shows a high tunneling magnetoresistance ratio, and could be the building block of a new class of spintronic devices. © *2011 American Institute of Physics.* [doi:10.1063/1.3562375]

I. INTRODUCTION

ZnO has been regarded as a key technological material for the future nanoscale electronic and optical devices due to its wide bandgap, piezoelectronic properties, and unique ability to form various types of nanostructures such as nanowires, nanobelts, nanotubes, nanosprings, nanorings, and many others.[1–3] Among all those nanostructures, ZnO nanowires are particularly interesting. Recent developments in experimental techniques have made possible the nice experimental control of the diameter, the crystalline direction, and the alignment of ZnO nanowires.[1] Based on these, the successful growth and control of the ZnO-nanowire array or network have also been demonstrated in recent experiments.[4] Large number of electronic and photonic devices based on ZnO nanowires have been proposed, such as field-effect transistors,[5] transparent electrodes for solar cells,[6] light-emitting devices,[7] and electricity nanogenerators.[8] All these applications make use of the wide energy bandgap or piezoelectric properties of ZnO nanowires. In current work, via first-principles investigations, we investigate the magnetic properties of C-doped ZnO nanowires and their applications for nanospintronic devices.

Chemical doping is a key technological process in materials science that has been widely used to fabricate hybrid materials with unique properties and functions. In the field of dilute magnetic semiconductors, magnetic properties of doped oxide bulk materials have been extensively studied. Strong magnetic moments in different oxide bulk materials induced by the doping of either magnetic or nonmagnetic elements have been reported both theoretically and experimentally in literature.[9–13] Quite recently, the doping-induced magnetism in quasi-1d semiconducting nanowires (SC-NWs) attracted considerable attention due to the great potential of applications of SC-NWs for the next generation of electronic or spintronic devices.[14–20] These studies have been focused on the effects of transition-metal doping on the magnetic properties of SC-NWs. To the best of our knowledge, nontransition-metal-doping-induced magnetism in ZnO nanowires has not been discussed so far, and despite the importance of oxide nanowires in real applications, a realistic prototype of an oxide-nanowire-based nanospintronic device is still missing.

In this work, via first-principles calculations based on density functional theory (DFT) and nonequilibrium Green's functions (NEGF) techniques, we show that the doping of C atoms can induce strong magnetic moments in ZnO nanowires, and the electronic structures as well as the magnetic properties of C-doped ZnO nanowires sensitively depend on partial hydrogenation. Based on these, we proposed a novel type of quasi-1d tunneling magnetic junctions (TMJs) made of partially hydrogenated C-doped ZnO nanowires. The proposed TMJ was found to have high tunneling magnetoresistance (TMR) ratio (86.7%). Unlike conventional TMJs consisting of two ferromagnetic (FM) electrodes and a non-magnetic center which are usually made of different materials, the proposed TMJ is made of a single material, therefore avoided the great difficulty in real applications of controlling the atomic structures of the contacts between different materials that often have important effects on performance of the device.[21] Also, for conventional TMJs, the TMR comes from unbalanced occupation of spin-up and spin-down channels around Fermi energy in two leads. As a result, reasonably high magnetic moments of two leads are normally necessary for high TMR ratio.[22] The origin of the high TMR ratio in the proposed TMJ is its unique magnetic interfaces between the center and two leads. Therefore, the strength of magnetic

a)Electronic mail: phyzc@nus.edu.sg.

moments of two leads is not essential for high TMR ratio. The proposed TMJ could form the basis of a new class of nanoscale spintronic devices.

II. COMPUTATIONAL METHODS

Our first-principles electronic structure calculations are based on DFT using SIESTA,[23] and the spin-dependent transport calculations were done by NEGF via the ATK package.[24,25] All calculations were performed using a double zeta polarized basis and norm-conserving pseudopotentials of the Troullier–Martin's type.[26] The generalized gradient approximation in Perdew–Burke–Ernzerhof format[27] was included. The atomic structures are optimized using the conjugate gradient method until the Hellman–Feynman force was "smaller" than 0.004 eV/Å. A vacuum region of at least 12 Å; between the nanowire and its replica due to periodic boundary conditions was employed to avoid the unnecessary interactions.

III. RESULTS AND DISCUSSION

First, we examined the electronic properties of pristine ZnO nanowires. Two nanowires along the experimentally often used [0001] direction with different diameters (7.7 and 11.3 Å) were considered in this paper. Cross sections of these two nanowires are shown in Figs. 1(a) and 1(c), respectively. The similar geometry of ZnO nanowires has been observed in experiments.[3] Both nanowires are nonmagnetic semiconductors. Our DFT calculations showed that the bandgap of the "bigger" one is about 1.64 eV, and the smaller one has a bigger bandgap 1.80 eV due to the stronger confinement originating from the smaller diameter. These results are consistent with previous theoretical results.[28,29]

We then considered the doping of carbon atoms. Previous theoretical studies have shown that for ZnO network, the doping of C atoms likely happens by substituting O atoms.[30] In one supercell of ZnO nanowires under study, there are four inequivalent doping sites for the smaller wire and six inequivalent doping sites for the bigger one, as shown in Figs. 1(b) and 1(d), respectively. To gain insights in effects of carbon doping on electronic properties of ZnO nanowires, first, we investigated the single carbon doping in one supercell of the smaller nanowire. The length of the supercell along the wire axis as shown in Fig. 2 is 10.7 Å. In this case, the coupling between C atoms in neighboring supercells can be neglected. In Figs. 1(a)–1(d), we show optimized structures of four possible configurations of single carbon-doped nanowires, respectively. With a single carbon doping, the nanowire is still a semiconductor with a smaller bandgap around 0.60 eV. Interestingly, for each of these four cases, the doping of a single carbon atom induces around 2 μ_B of magnetic moment in the supercell. As shown in the figure, the spin charge density defined as the difference between charge densities of two spin channels is mainly centered on the doped carbon atom, spreading to neighboring O atoms. Detailed analysis of partial density of states (DOS) revealed that the spin polarization originates from the unbalanced occupation of spin-up and spin-down channels of carbon p orbitals due to the interac-
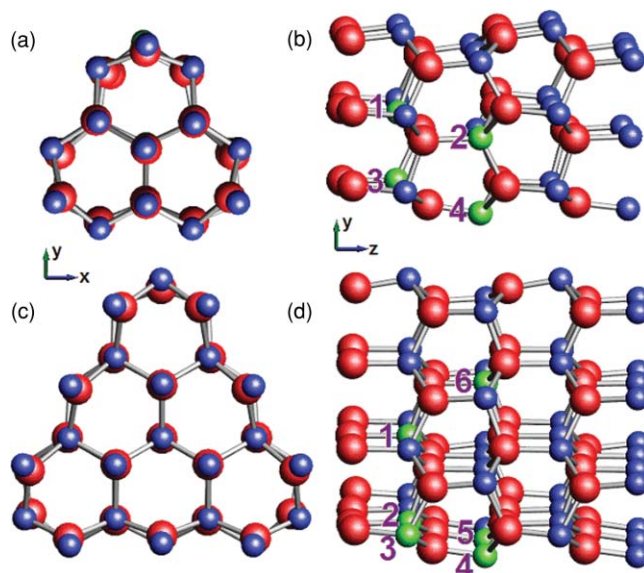

FIG. 1. Atomic configurations and possible carbon doping sites of ZnO [0001] nanowires enclosed by (10$\bar{1}$0) surfaces. Color scheme: Zn in red, O in blue, and possible C doping sites in green. (a) Cross section of smaller nanowire with the diameter 7.7 Å. (b) Side view of the smaller wire. There are four possible C doping sites. (c) Cross section of ``bigger" nanowire with the diameter 11.3 Å. (d) Side view of the bigger wire. There are six possible C doping sites.

tion between the carbon and the closest neighboring oxygen atoms. In particular, when the carbon atom is doped in the position 1 [center position, Fig. 2(a)], the closest O atoms are in x–y plane. The interaction between the C atom and these O atoms results in unoccupied spin-down p_x and p_y orbitals of carbon as we can see from partial DOS [Fig. 2(e)], leading to a 2 μ_B of magnetic moment; when the carbon atom is
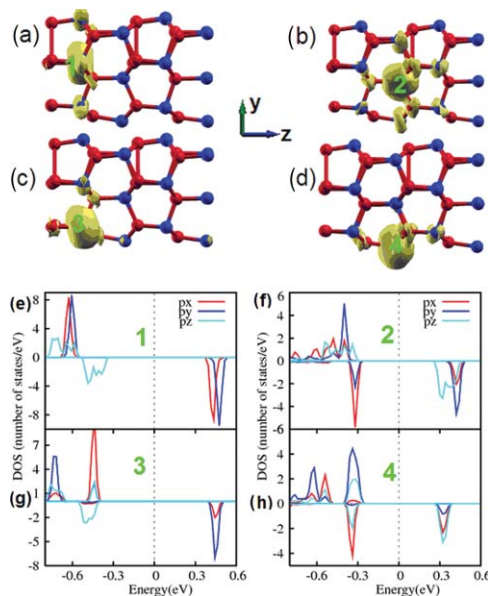

FIG. 2. Doping of single carbon in one supercell of the smaller ZnO nanowires. Color scheme is the same as Fig. 1. (a)–(d) show the spin density defined as the difference between the spin-up and spin-down charge densities for the four possible C doping sites, respectively, and (e)–(h) are the corresponding partial DOS of the C atom for these four configurations.

doped in position 2 [Fig. 2(b)], the C atom interacts with O atoms in all three directions. Therefore, the magnetic moment comes from unoccupied spin-down channel of all three p orbitals of carbon [Fig. 2(f)]; for the case of doping in position 3 [Fig. 2(c)], the closest O atom is right above C in x and y directions, resulting in unoccupied spin-down p_x and p_y orbitals [Fig. 2(g)]; for the case of doping in position 4 [Fig. 2(d)], for the same reason, the magnetic moment mainly comes from unoccupied spin-down p_y and p_z orbitals of carbon [Fig. 2(h)].

Next, we considered the doping of two carbon atoms in one supercell for which the coupling between two spin-polarized carbon atoms has to be taken into account. Among all combinations of possible doping sites as shown in Fig. 1, for the smaller nanowire, the lowest energy state turns out to be the FM coupling configuration as shown in Fig. 3(a) for which one carbon atom doped in the center position and the other one in surface position [positions 1 and 3 in Fig. 1(b), respectively], and for the bigger nanowire, two carbon atoms prefer to substitute O atoms in two surface positions [positions 3 and 4 in Fig. 1(d)] with FM coupling as shown in Fig. 3(b). It is worthy mentioning here that with two carbon atoms, the nanowire is still a semiconductor with a further decreased bandgap around 0.5 eV. Similar to the single carbon doping, the spin polarization originates from interaction between carbon atoms and nearby oxygen atoms. For the smaller one, as shown in Fig. 3(c), for both carbon atoms, due to the substitution of one oxygen atom in y direction, the contribution of p_y orbital to the spin polarization is significantly suppressed, and the magnetic moment in this case mainly comes from unoccupied p_x orbital. Each of these two carbon atoms contributes around 1 μ_B of magnetic moment. For the bigger nanowire, the magnetic moment is mainly centered at the carbon atom 1 that contributes around 1.56 μ_B of magnetic moment. The second carbon atom has near 0.15 μ_B of moment. O atoms surrounding the carbon atom 1 overall also

FIG. 4. (a) Cross section of fully hydrogenated C-doped ZnO nanowire. H atoms are in white. H atoms are divided into six layers as shown in the figure. (b) The change of magnetic moment when the system is hydrogenated layer by layer.

contribute near 0.18 μ_B of moment. In this case, for carbon atom 1, the interaction with nearby O atoms (in x and y directions) is essential, which leads to the major contribution of p_x and p_y orbitals to the spin polarization [Fig. 3(d)].

We next investigate the effects of partial hydrogenation on electronic and magnetic properties of C-doped ZnO nanowires. It has been reported in literature that the hydrogen passivation has important effects on properties of SC-NWs.[29] In particular, for ZnO nanowire, a recent theoretical study showed that a 50% of hydrogen passivation may turn ZnO nanowire from semiconductor to metal.[29] As shown in Fig. 4(a), we chose the lowest energy state of two-carbon-doped bigger ZnO nanowire as a case study. The outermost oxygen atoms are chosen to be possible adsorption sites of hydrogen atoms. We divided these possible adsorption sites into six layers [see Fig. 4(a)] and hydrogenate the wire layer by layer starting from layer 1. Our calculations suggested that for C-doped ZnO nanowire, both the bandgap and the magnetic moment sensitively depend on the coverage of H atoms. The bandgap disappears when the layer 1 is hydrogenated. The magnetic moment decreases to about 0.2 μ_B at around 60% of coverage and when fully hydrogenated, the wire is nonmagnetic.

Based on aforementioned findings, we propose a possible quasi-1d TMR junction made of a partially hydrogenated C-doped ZnO nanowire as shown in Fig. 5(a). The lowest energy state of two-carbon-doped smaller ZnO wire [Fig. 3(a)] is chosen for this study due to the limited computational power. One $(10\bar{1}0)$ surface of both left and right semi-infinite electrodes is passivated by H as shown in the figure. The partial hydrogenation of the $(10\bar{1}0)$ surface of ZnO has been demonstrated in recent experiments.[31,32] The center region (device region) consists of one unit cell of each electrode and one unit cell of unpassivated C-doped wire [Fig. 3(a)]. This could be done in experiment using a mask in the center region during the hydrogenation process. Our calculations based on nudged elastic band[33] method show that the diffusion barrier of one H atom from one O atom to another one is around 2.5 eV, so at room temperature, H atoms are not able to diffuse from electrodes to the center region. In Fig. 5(b), we show the total density of states of both spin-up and spin-down channels for partially hydrogenated electrodes. As shown in the figure, two electrodes are metallic, which is consistent with our discussion in the previous paragraph that a small coverage of
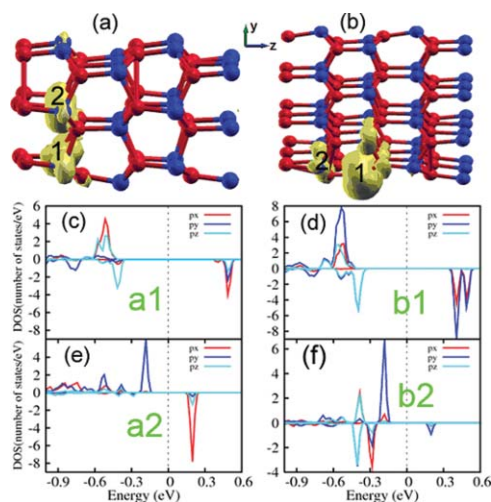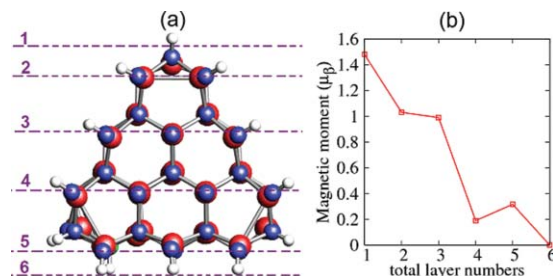

FIG. 3. Lowest energy states and partial DOS of two-carbon doping in ZnO nanowires. (a) Two-carbon doping in the smaller wire. (b) Two-carbon doping in the bigger wire. (c) and (e) are partial DOS of two carbon atoms in the configuration shown in (a) [a1 denotes the first C atom in (a) and a2 denotes the second C atom]. (d) and (f) show partial DOS of two carbon atoms in the bigger wire.
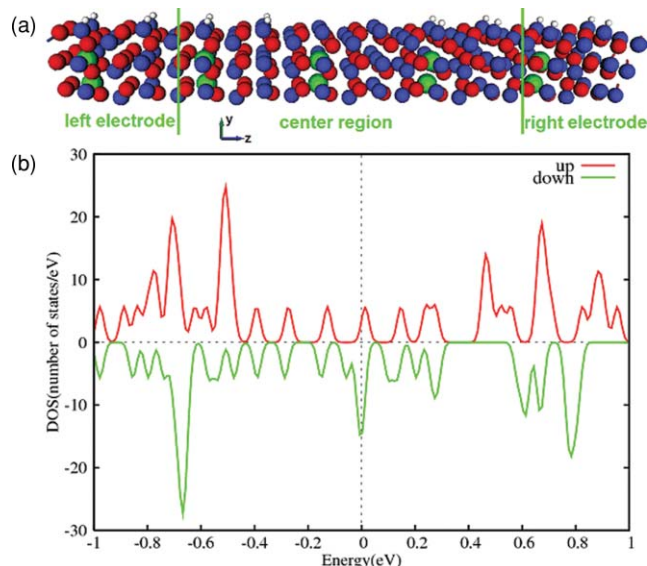
FIG. 5. A possible quasi-1d TMR junction made of a partially hydrogenated C-doped ZnO nanowire. The color scheme is the same as before. (a) The atomic configuration of the junction. Two electrodes are semi-infinite partially hydrogenated C-doped ZnO wires. The center region contains one unit cell of unhydrogenated wire and one unit cell of each electrode. (b) Spin-resolved total density of states of partially hydrogenated electrodes. Clearly, the partial hydrogenation turns the wire from semiconductor to metal.

H atoms can turn the C-doped ZnO wire from semiconductor to metal. The magnetic moment in one unit cell for this case is estimated to be 0.5 μ_B, which is relatively low, compared to 2 μ_B of magnetic moment in the unpassivated part of the center region, and agrees with our calculations for bigger nanowire that the magnetic moment of the wire decreases when hydrogenated. Unlike the conventional TMJs consisting of two magnetic electrodes and one nonmagnetic center which has two magnetic configurations, parallel and antiparallel, The TMJ shown in Fig. 5(a) has three different magnetic configurations, (111), (110), and (101), where three numbers in the bracket denote directions of magnetic moments of left electrode, center region, and right electrode, respectively, with the number 1 representing up direction and number 0 representing down direction. We then calculated the equilibrium conductance of both spin channels for all these three magnetic configurations using the first-principles approach combining spin-polarized DFT and NEGF. For (101) configuration, the conductance for both spin channels is essentially zero. Also considering the fact that it is very difficult, if not impossible, to control the magnetic moment in atomic scale using external field so that the magnetic configuration (101) is not practical, we calculate the TMR ratio of the junction using the conductance of (111) and (110) only by TMR = (G_{111} − G_{110})/G_{111}. Spin-dependent conductances for these two configurations are listed in Table I. From the table, we can see that the spin-up channel of (111) configuration is open with a conductance around 0.13 G_0, and other channels are essentially close with quite low conductance. The TMR ratio is estimated to be 86.7%.

To further understand the origin of the high TMR ratio, we plotted isosurfaces of spin-resolved local density of states (LDOS) at Fermi energy for both (111) and (110) con-

TABLE I. The equilibrium conductance of both spin channels for (111), (110) magnetic configurations.

Configuration Conductance (G_0)	(111)	(110)
Majority channel (spin-up)	0.128	0.015
Minority channel (spin-down)	0.007	0.003
Total	0.135	0.018

figurations in Fig. 6. For (111) configuration [Figs. 6(a) and 6(b)], the nice electronic connection between electrodes and the center region for spin-up electrons [Fig. 6(a)] suggests the open of this channel, and the lack of LDOS for spin-down electrons in the center region is the origin of the close of this channel. For (110) configuration [Figs. 6(c) and 6(d)], spin-up electrons have no problem to propagate from left electrode to the center region through the left contact, while, in the right contact, the spin-up LDOS is clearly disconnected, suggesting a strong reflection of spin-up electrons at the right interface; for spin-down channel, on the contrary, the LDOS suggests a strong reflection at the left interface.

Since in reality, spintronic devices always operate under a small finite bias, we also calculated the current as a function of bias voltages for both (111) and (110) configurations. Results are shown in Fig. 7. TMR as a function of bias voltage is defined as (I_{par} − I_{anti})/I_{par}, where I_{par} denotes the current for the configuration (111), and I_{anti} is the current for the configuration (110). As shown in the figure, the TMR is quite high, around 40% when the bias is smaller than 0.1 V, and then drops quickly from around 40% to 20% when the bias varies from 0.1 to 0.2 V. The change of TMR as a function of bias for this quasi-1d device is similar to that of conventional bulk TMR devices consisting of two different materials where it is found that a small bias around 0.2 V greatly decreases the TMR.[34,35]
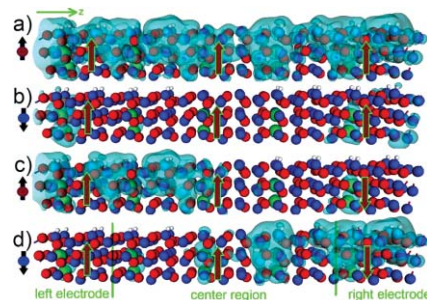

FIG. 6. Isosurface of LDOS at Fermi energy for different spin channels and magnetic configurations. The shorter (black) arrow at the left side of each panel denotes the spin channel of electrons. Three longer (red) arrows in each panel denote the orientation of the magnetic moment of the left electrode, center region, and right electrode, respectively. (a) LDOS of the spin-up channel (majority spin channel) of (111) configuration. (b) LDOS of the spin-down channel (minority spin channel) of (111) configuration. (c) LDOS of the spin-up channel of (110) configuration. (d) LDOS of the spin-down channel of (110) configuration.
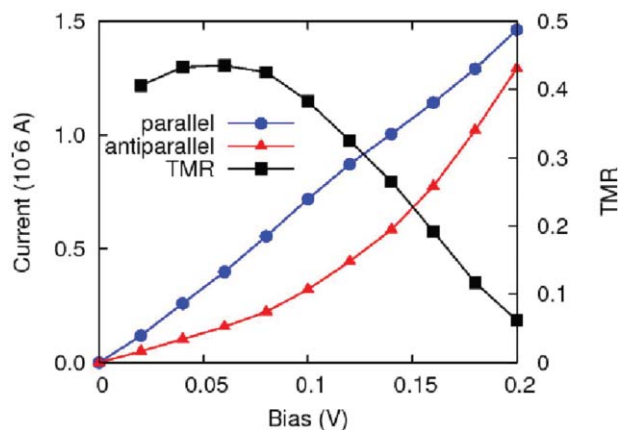
FIG. 7. Current and TMR as functions of bias voltage for the device as shown in Fig. 5(a) TMR here is defined as $(I_{par} - I_{anti})/I_{par}$, where I_{par} denotes the current for the configuration (111), and I_{anti} is the current for the configuration (110).

IV. CONCLUSION

In summary, in this paper, we investigated electronic structures, magnetic properties, and spin-dependent electron transport characteristics of C-doped ZnO nanowires via first-principles method based on DFT and NEGF. Our calculations show that the doping of carbon atoms in a ZnO nanowire could induce strong magnetic moments in the wire, and the electronic structures as well as the magnetic properties of the system sensitively depend on partial hydrogenation. Based on these findings, we proposed a quasi-1d TMJ made of a partially hydrogenated C-doped ZnO nanowire, which shows a high TMR ratio. The proposed TMJ has several obvious advantages compared to conventional TMJs consisting of two magnetic electrodes and on nonmagnetic center. First, the proposed TMJ is made of a single material, therefore avoided the great difficulty of controlling the contact structure between different materials. Second, the origin of TMR of the proposed TMJ is the unique magnetic interface between electrodes and device region, so the strong magnetic moment in two electrodes may not be necessary for high TMR ratio. Because of these, the proposed TMJ could be the building block of a new class of spintronic devices.

ACKNOWLEDGMENTS

[1] Z. L. Wang, Mater. Sci. Eng. R. **64**, 33 (2009).
[2] X. D. Wang, J. H. Song, and Z. L. Wang, J. Mater. Chem. **17**, 711 (2007).
[3] X. Wang, J. Song, and Z. L. Wang, Chem. Phys. Lett. **424**, 86 (2006).
[4] G. D. Yuan, W. J. Zhang, J. S. Jie, X. Fan, J. A. Zapien, Y. H. Leung, L. B. Luo, P. F. Wang, C. S. Lee, and S. T. Lee, Nano Lett. **8**, 2591 (2008).
[5] W. Hong, G. Jo, J. I. Sohn, W. Park, M. Choe, G. Wang, Y. Kahng, M. Welland, and T. Lee, ACS Nano **4**, 811 (2010).
[6] B. D. Yuhas and P. D. Yang, J. Am. Chem. Soc. **131**, 3756 (2009).
[7] E. Lai, W. Kim, and P. D. Yang, Nano Res. **1**, 123 (2008).
[8] Z. L. Wang and J. H. Song, Science **312**, 242 (2006).
[9] H. Pan, J. B. Yi, L. Shen, R. Q. Wu, J. H. Yang, J. Y. Lin, Y. P. Feng, J. Ding, L. H. Van, and J. H. Yin, Phys. Rev. Lett. **99**, 127201 (2007).
[10] B. David and G. Emmanuel, J. Phys.: Condens. Matter **19**, 236224 (2007).
[11] T. Dietl, H. Ohno, F. Matsukura, J. Cibert, and D. Ferrand, Science **287**, 1019 (2000).
[12] J. B. Yi, C. C. Lim, G. Z. Xing, H. M. Fan, L. H. Van, S. L. Huang, K. Yang, X. Huang, X. Qin, B. Wang, T. Wu, L. Wang, H. Zhang, X. Gao, T. Liu, Q. Wee, Y. Feng, and J. Ding, Phys. Rev. Lett. **104**, 137201 (2010).
[13] K. Yang, R. Q. Wu, L. Shen, Y. P. Feng, Y. Dai, and B. B. Huang, Phys. Rev. B **81**, 125211 (2010).
[14] H. J. Xiang and S. H. Wei, Nano Lett. **8**, 1825 (2008).
[15] D. Q. Gao, Y. Xu, Z. H. Zhang, H. Gao, and D. S. Xue, J. Appl. Phys. **105**, 63903 (2009).
[16] Q. Wang, Q. Sun, P. Jena, and Y. Kawazoe, Nano Lett. **5**, 1587 (2005).
[17] D. Q. Gao, D. S. Xue, Y. Xu, Z. J. Yan, and Z. H. Zhang, Electrochim. Acta **54**, 2392 (2009).
[18] P. V. Radovanovic, C. J. Barrelet, S. Gradeak, F. Qian, and C. M. Lieber, Nano Lett. **5**, 1407 (2005).
[19] G. Giorgi, X. Cartoixa, A. Sgamellotti, and R. Rurali, Phys. Rev. B **78**, 115327 (2008).
[20] S. Xu, Y. Qin, C. Xu, Y. G. Wei, R. S. Yang, and Z. L. Wang, Nat. Nanotechnol. **5**, 366 (2010).
[21] X. G. Zhang, W. H. Butler, and A. Bandyopadhyay, Phys. Rev. B **68**, 92402 (2003).
[22] C. Zhang, L. L. Wang, H. P. Cheng, X. G. Zhang, and Y. Xue, J. Chem. Phys. **124**, 201107 (2006).
[23] J. M. Soler, E. Artacho, J. D. Gale, A. García, J. Junquera, P. Ordejón, and D. S. Portal, J. Phys.: Condens. Matter **14**, 2745 (2002).
[24] M. Brandbyge, J. L. Mozos, P. Ordejón, J. Taylor, and K. Stokbro, Phys. Rev. B **65**, 165401 (2002).
[25] J. Taylor, H. Guo, and J. Wang, Phys. Rev. B **63**, 245407 (2001).
[26] N. Troullier and J. L. Martins, Phys. Rev. B **43**, 1993 (1991).
[27] J. P. Perdew, K. Burke, and M. Ernzerhof, Phys. Rev. Lett. **77**, 3865 (1996).
[28] B. L. Wang, J. J. Zhao, J. M. Jia, D. N. Shi, J. G. Wan, and G. H. Wang, Appl. Phys. Lett. **93**, 21918 (2008).
[29] H. Xu, A. L. Rosa, T. Frauenheim, R. Q. Zhang, S. T. Lee, and Ch. Wöll, Appl. Phys. Lett. **91**, 31914 (2007).
[30] B. J. Nagare, S. Chacko, and D. G. Kanhere, J. Phys. Chem. A **114**, 2689 (2010).
[31] K. Ozawa and K. Mase, Phys. Status Solidi A **207**, 277 (2010).
[32] Y. Wang, B. Meyer, X. Yin, M. Kunat, D. Langenberg, F. Traeger, A. Birkner, and Ch. Wöll, Phys. Rev. Lett. **95**, 266104 (2005).
[33] G. Mills, H. Jonsson, and G. K. Schenter, Surf. Sci. **324**, 325 (1995).
[34] C. Zhang, X.-G. Zhang, P. S. Krstić, H.-P. Cheng, W. H. Butler, and J. M. MacLaren, Phys. Rev. B **69**, 134406 (2004).
[35] D. Waldron, V. Timoshevskii, Y. Hu, K. Xia, and H. Guo, Phys. Rev. Lett. **97**, 226802 (2006).